Environmental Science & Technology

pubs.acs.org/est

Article

Co-Exposure of Ambient Particulate Matter and Airborne Transmission Pathogens: The Impairment of the Upper Respiratory Systems

Yu Qi,* Yucai Chen, Xu Yan, Wei Liu, Li Ma, Yongchun Liu, Qingxin Ma, and Sijin Liu

Cite This: *Environ. Sci. Technol.* 2022, 56, 15892−15901

Read Online

ACCESS | Metrics & More | Article Recommendations | Supporting Information

ABSTRACT: Recent evidence has pinpointed the positive relevance between air particulate matter (PM) pollution and epidemic spread. However, there are still significant knowledge gaps in understanding the transmission and infection of pathogens loaded on PMs, for example, the interactions between pathogens and pre-existing atmospheric PM and the health effects of co-exposure on the inhalation systems. Here, we unraveled the interactions between fine particulate matter (FPM) and *Pseudomonas aeruginosa* (*P. aeruginosa*) and evaluated the infection and detrimental effects of co-exposure on the upper respiratory systems in both in vitro and in vivo models. We uncovered the higher accessibility and invasive ability of pathogens to epithelial cells after loading on FPMs, compared with the single exposure. Furthermore, we designed a novel laboratory exposure model to simulate a real co-exposure scenario. Intriguingly, the co-exposure induced more serious functional damage and longer inflammatory reactions to the upper respiratory tract, including the nasal cavity and trachea. Collectively, our results provide a new point of view on the transmission and infection of pathogens loaded on FPMs and uncover the in vivo systematic impairments of the inhalation tract under co-exposure through a novel laboratory exposure model. Hence, this study sheds light on further investigations of the detrimental effects of air pollution and epidemic spread.

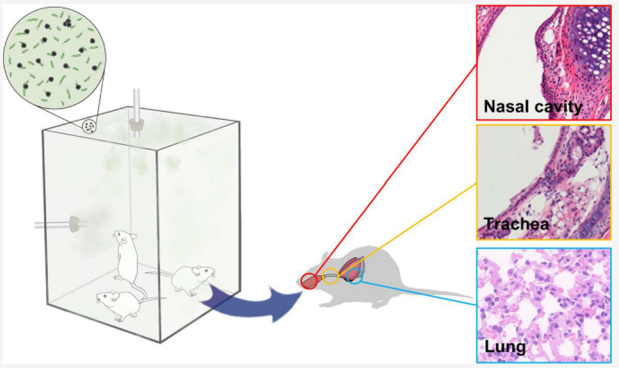

KEYWORDS: *particulate matter, pathogens, inhalation system, upper respiratory tract, inflammation*

INTRODUCTION

Air pollution poses an outstanding challenge to public health and even pathogen epidemics.[1−3] Particulate matter (PM), a particulate component of air pollution, can increase the occurrence of various detrimental health effects.[2,4−6] Recently, mounting data have evidenced the implications of PMs in pathogen (e.g., bacteria and viruses) transmission and epidemic spreading.[3,7−10] For instance, many epidemiological studies have suggested that PM pollution is positively correlated to clinical influenza-like illness, active tuberculosis, and even the 2019 novel coronavirus (SARS-CoV-2).[11−14] Of note, it has also been proposed that pathogens, such as bacteria, fungi, and viruses, could attach to dust particles or tiny droplets as bioaerosols.[8,12,15−17] Although a large amount of evidence indicates the possibility for pathogens traveling and transmitting through hitchhiking with PMs, much less is understood regarding the co-exposure of PMs and pathogens. In fact, numerous questions need to be answered, that is, how pathogens load on PMs, whether the co-exposure of PMs and pathogens together would induce more severe detrimental effects, and what are the long-term effects of co-exposure to PMs and pathogens together on the respiratory system. To illustrate the scale of the questions, it would be of great significance to fill these knowledge gaps on pathogen loading on PMs and their health risks.

While many recent studies have debated the existence of viruses, especially SARS-CoV-2, on atmospheric PMs,[18−21] other kinds of pathogens, such as bacteria and fungi, could be detected in PMs.[22−24] To date, an increasing number of studies have pointed out that bacteria in the atmosphere can enter the human body through the respiratory tract, posing threats to human health and causing serious public health problems, including infections, acute toxic effects, allergies, and even cancers.[22,23,25] At present, many studies have focused on the relationships between PMs, especially fine particulate matters (FPMs), and bacterial infection of the lung.[26−31] For

Received: May 30, 2022
Revised: October 4, 2022
Accepted: October 4, 2022
Published: October 14, 2022

https://doi.org/10.1021/acs.est.2c03856
Environ. Sci. Technol. 2022, 56, 15892−15901

example, Mushtaq et al. found that FPMs could facilitate bacteria adherence to lower airway cells and increase the vulnerability of cells.[26] Liu et al. proposed that exposure to FPMs promoted ROS generation in lung epithelial cells and disrupted the epithelial barrier, leading to the invasion of *Pseudomonas aeruginosa* (*P. aeruginosa*).[28] Shears et al. suggested that exposure to diesel exhaust particles would retard the phagocytic function of alveolar macrophages and increase *pneumococcal* infections in the lung.[30] Despite these mechanisms, several puzzles remain to be figured out. First, the exposure procedures of recent studies often administrated PMs and bacteria separately.[3,28,30] The exposure mode simulates the separate scenarios, namely, the damage to the respiratory system after PM pollution and, per se, the defense against pathogen invasion. Under this premise, here is limited understanding of the scenario of co-exposure to PMs and pathogens as well as the related detrimental effects, which need to be elucidated. In addition, most studies have focused on the health effects of the lung because the lungs are commonly regarded as the first target organs.[4] The defensive role of the upper respiratory tract against exotic invaders has been largely omitted. In fact, the upper respiratory tract plays an important role in defense and clearance of exotic invaders such as FPMs and pathogens. Therefore, the effects of co-exposure on the upper respiratory tracts warrant detailed investigation.

To solve the above questions, we scrutinized the interaction between various FPMs and one typical respiratory pathogen, that is, *P. aeruginosa*, and the in vitro invasive ability to epithelial cells. In addition, to understand the health risks upon co-exposure in vivo, a chamber for animal experiments was designed by generating several airflows for inhalation exposure under various conditions. Based on the designed inhalation exposure model, impairments in the upper respiratory system were further investigated. Together, our combined results systematically unraveled the detrimental effects of co-exposure to FPMs laden with pathogens on the upper respiratory system as well as the whole body.

MATERIALS AND METHODS

Bacterial Strain. *P. aeruginosa* was obtained and maintained with approval from the Ethics Committee at the Research Center for Eco-Environmental Sciences, Chinese Academy of Sciences (Beijing, China). Bacterial cell growth efficacy was determined through growth curves reflective of absorption at OD_{600} and colony forming unit (CFU) counting. Plasmid pMF230 was a gift from Michael Franklin (Addgene plasmid # 62546; http://n2t.net/addgene:62546; RRID: Addgene_62546).[32]

FPM Preparation and Characterization. The ultrafine test dust sample (i.e., dust) was purchased from Powder Technology Incorporated (USA).[33] The SiO_2 and Al_2O_3 particles were purchased from Sigma-Aldrich (USA). Black carbon (BC) particles were combusted from corn straw under oxygen-limited conditions at 600 °C. The obtained biochar was crushed in deionized (DI) water, and the fractions that passed through a 3 μm sieve were collected using 0.22 μm filters and then dried at 105 °C for 48 h. The collected BC particles were then applied for further experiments. The fluorescent polystyrene (FPS) particles were purchased from Baseline, Inc. (China). The physical dimensions and morphology of these FPMs and the interaction between FPMs and *P. aeruginosa* were characterized by scanning electron microscopy (SEM, SU-8020, Hitachi, Germany).

Cell Culture and Cytotoxicity Assessment. Epithelial A549 cells were purchased from the Shanghai Cell Bank of Type Culture Collection (China) and were cultured in Dulbecco's modified Eagle medium (DMEM) supplemented with 10% fetal bovine serum (FBS, Gibco, USA) and 100 U/mL penicillin−streptomycin (HyClone, USA). Cells were cultured at 37 °C in a humidified incubator with 5% CO_2. For cytotoxicity assessment, A549 cells were treated with FPMs at various concentrations for 24 h after seeding in a 96-well (Corning, USA) plate overnight. Cytotoxicity was then assayed using a Cell Counting Kit-8 (CCK-8) following the standard manufacturer's instructions (Solarbio, China).

Molecular Dynamics Simulations. Briefly, the CHARMM36 all-atom (AA) force field[34] and INTERFACE force field[35] were used to capture the interactions of the Gram-negative bacterial outer membrane (lipopolysaccharide, LPS and 1-palmitoyl-2-oleoyl-phosphatidylethanolamine, POPE)[36] with materials including SiO_2, carbon base, polystyrene, and Al_2O_3. The crystal structures for these materials were adopted from the Materials Project.[37] The $x-y$ dimensions of the simulation boxes were fixed at 8 nm × 8 nm, and periodic boundary conditions were applied to all dimensions (namely, the surface was infinite in $x-y$ dimensions). Each of the simulation systems went through a 20 ns production run with a time step of 2 fs and GROMACS software (version 2019.6) after a 5 ns pre-equilibrium process.

Bacterial Invasion Assay. A549 cells were seeded into 12-well plates (Corning, USA) overnight. The FPMs in phosphate-buffered saline (PBS) at various concentrations were first incubated with *P. aeruginosa* at multiplicities of infection (MOI) of 10 for 30 min at 37 °C (OD_{600} 0.25 = 1 × 10^8 CFU/mL). Then, the medium of the cells was replaced by the medium with DMEM containing the corresponding concentrations of particles and bacterial suspension for 4 h at 37 °C and 5% CO_2. After that, the supernatants were removed, and the cells were washed 3 times with PBS. In addition, 200 μg/mL gentamicin sulfate (Sigma-Aldrich, USA) was added to the wells and incubated for another 2 h to eliminate the extracellular bacteria. Subsequently, the cells were washed 5 times with PBS and lysed with 0.1% Triton X-100 (Sigma-Aldrich, USA). The lysates were then serially diluted and plated onto agar plates with ampicillin in triplicate. The numbers of invasive bacteria were counted according to the CFU.

Bacteria Adhesion Assay. The adhesion of *P. aeruginosa* to A549 cells was assessed by using a standard bacterial adhesion assay.[26] Briefly, A549 cells were seeded into 12-well plates (Corning, USA) overnight. The FPMs at various concentrations (i.e., 5, 10, and 50 μg/mL) were first incubated with *P. aeruginosa* at an MOI of 10 for 30 min at 37 °C. Then, the medium of the cells was replaced by the medium with DMEM containing the corresponding concentrations of particles and bacterial suspension for 4 h at 4 °C. After that, cells were washed 5 times with PBS to remove loosely attached *P. aeruginosa*. Cells were then removed from the 12-well plates and lysed with 0.1% Triton X-100 (Sigma-Aldrich, USA), and the lysates were then serially diluted and plated onto agar plates with ampicillin in triplicate. The numbers of adherent bacteria were counted according to the CFU.

Chamber Operation. The main body of the chamber (250 × 250 × 350 mm) was constructed using acrylic. Briefly, particle (i.e., SiO_2) flow was generated using a small-scale powder disperser (3433, TSI, USA) and it maintained a steady

https://doi.org/10.1021/acs.est.2c03856
Environ. Sci. Technol. 2022, 56, 15892−15901

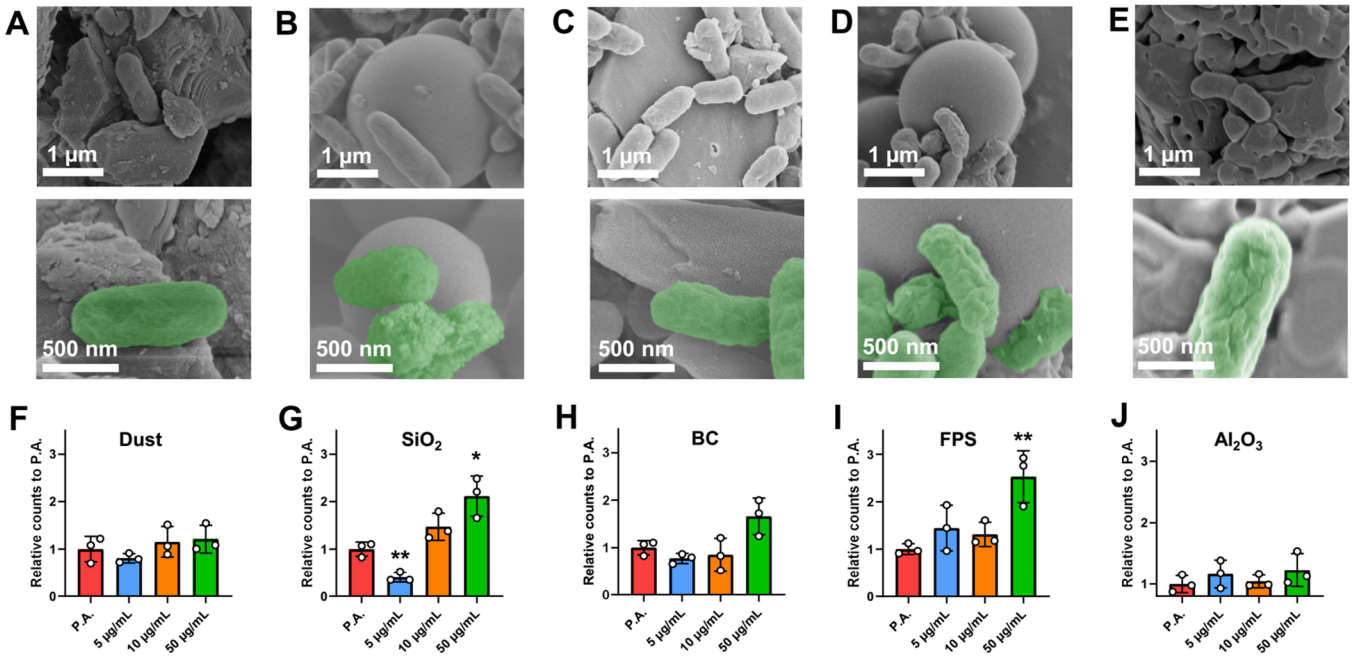

Figure 1. Characterization of the interaction between various FPMs and *P. aeruginosa*, and the co-exposure invasion ability to A549 cells. SEM images of the interaction between *P. aeruginosa* and dust (A), SiO_2 particles (B), BC particles (C), FPS (D), and Al_2O_3 particles (E). Invasion ability to A549 cells is evaluated followed by infection with *P. aeruginosa* and various FPMs (F–J). CFU counts are performed to determine the number of viable *P. aeruginosa*. Statistical significance between groups: (*) $P < 0.05$ and (**) $P < 0.01$.

concentration (i.e., ~38 ± 3 $\mu g/m^3$) in the chamber, monitored by DUSTTRACK DRX (8533, TSI, USA). The bacteria suspension was added to a modified nebulizer (NE-C900, Omron, China) to generate aerosol droplets containing bacteria. The mice were placed in the bottom of the chamber under various exposures.

Animal Experiments. BALB/c mice (male, 6–7 weeks old) were obtained from Vital River Laboratory Animal Technology Co., Ltd. (Beijing, China). All animal experimental protocols were approved by the Animal Ethics Committee at the Research Center for Eco-Environmental Sciences, Chinese Academy of Sciences (Beijing, China). All animals were housed and maintained in a specific pathogen-free (at the SPF grade) and aseptic animal facility. Mice were placed into the chamber for exposure under clean air, FPMs only (i.e., SiO_2), *P. aeruginosa* only, or co-exposure for 30 min. After that, the mice were sacrificed at various timepoints. Then, the nasal cavities, tracheas, lungs, and blood were collected. The tissues were fixed in PBS-buffered 10% formaldehyde solution, embedded in paraffin, and sliced into sections for hematoxylin–eosin (H&E) staining, following a standard procedure. The collected blood was analyzed by complete blood count (CBC) analysis. The nasal washes were collected by using PBS, further serially diluted, and then plated onto agar plates with ampicillin in triplicate. The numbers of loading bacteria were counted according to the CFU. The mucociliary clearance (MCC) was evaluated according to a method reported previously and through high-resolution live-cell confocal imaging microscopy (OLYMPUS IX83ZDC, Japan).[38]

Statistical Analysis. All data were shown as the mean ± standard deviation (SD) and were analyzed with GraphPad Prism software (version 8.0.2). The independent *t*-test was applied for comparisons between the control and different groups. $P < 0.05$ herein was considered statistically significant. Statistical significance between groups (*) $P < 0.05$, (**) $P < 0.01$, and (#) $P < 0.001$.

RESULTS AND DISCUSSION

FPMs Facilitate Pathogen Accessibility and Invasion to Epithelial Cells. The interaction and invasive ability of *P. aeruginosa* co-exposure with various FPMs on epithelial cells A549 were evaluated. Hereby, different types of FPMs, that is, dust, SiO_2 particles, BC, microplastic particles, and Al_2O_3 particles were chosen to represent the real FPMs because these compositions were commonly found in atmospheric environments.[3,39] The dust sample is a mixture of ambient fine particles containing silica (69–77%), aluminum oxide (8–14%), and other minerals taken from the real environment and is commonly applied to represent real PMs.[33] In addition, model FPMs with simple compositions, such as silica (SiO_2) particles, aluminum oxide (Al_2O_3) particles, and microplastics (fluorescent polystyrene) particles, were chosen to represent the real PMs according to the major components of dust samples and model FPMs applied in previous studies.[33,40,41] The SEM images showed that the five model particles appeared in different morphologies, but all had a size of approximately 2 μm (Figure S1), consistent with the size of real FPMs. In specific, the SiO_2 and FPS particles were spheres with smooth surfaces, and BC particles appeared as sheet-like morphologies. The dust and Al_2O_3 particles appeared as aggregates with amorphous morphologies.

Furthermore, the interactions between particles and *P. aeruginosa* were further characterized. After incubation for 30 min at 37 °C, the stably adhered bacteria on the surface of the particles were characterized, as shown in Figure 1A–E. Intriguingly, the interactions of *P. aeruginosa* with different particles were different. For example, because of the rough surface of dust and Al_2O_3, the bacteria tended to "scratch" on the relatively smooth part of the particles. In contrast, the

https://doi.org/10.1021/acs.est.2c03856
Environ. Sci. Technol. 2022, 56, 15892–15901

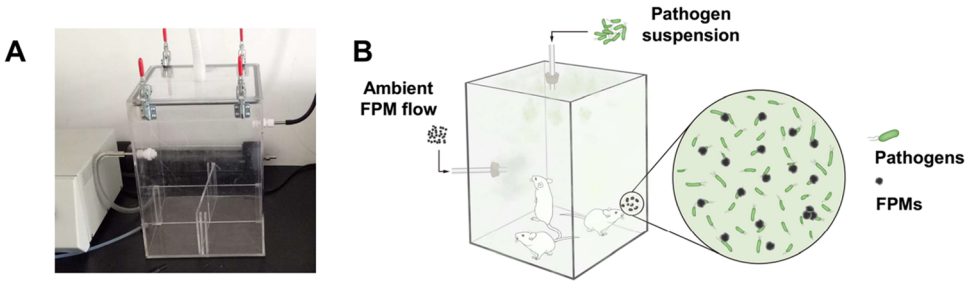

Figure 2. Laboratory co-exposure model and the inflammatory reaction of different exposure patterns. Photograph (A) and scheme (B) show the designed chamber for various exposure patterns, including FPMs/pathogens-only and co-exposure.

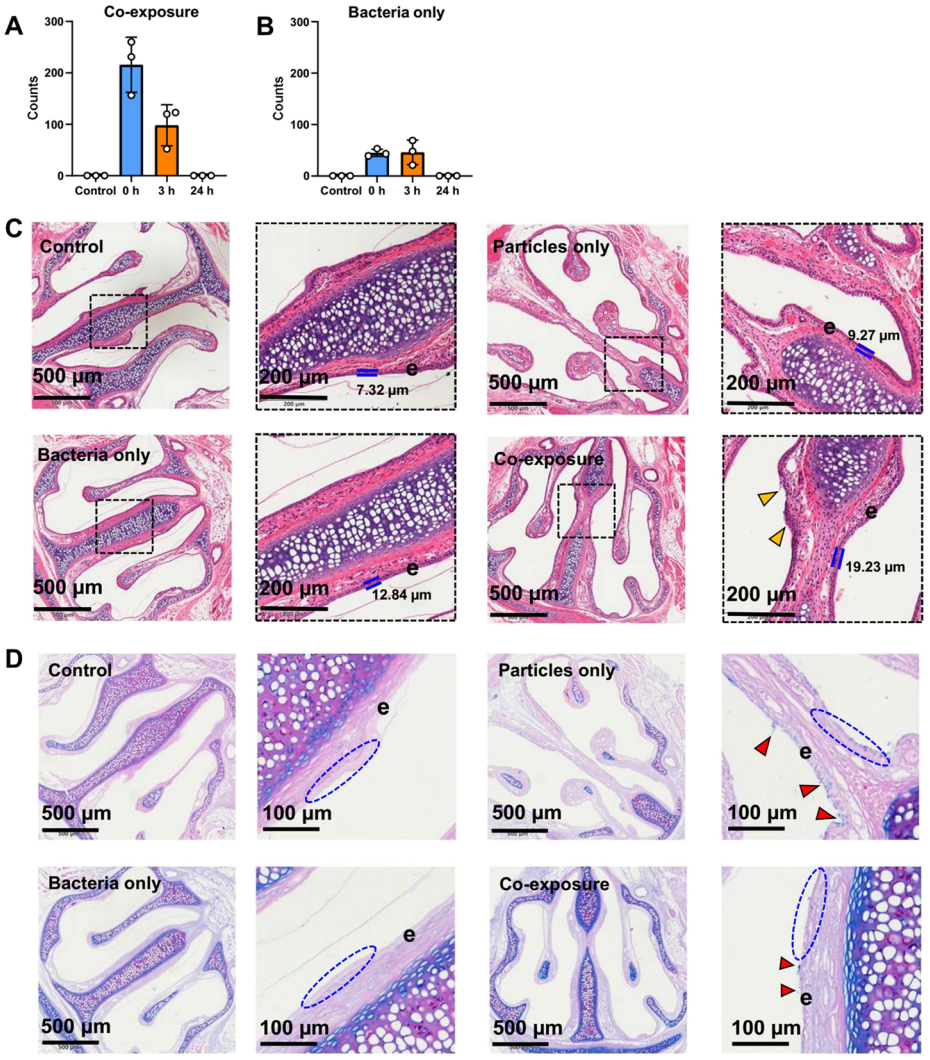

Figure 3. Histology and physiology of nasal cavity after various exposure patterns. Bacteria loading in nasal cavity after co-exposure (A) and bacteria-only exposure (B). (C) Histology stained with H&E of nasal cavity from mice exposed to clean air, FPMs-only, bacteria-only, and co-exposure for 30 min. Thickness of nasal transitional epithelium (e) is measured. Inflammatory cell influx is indicated by yellow arrowheads. (D) Histology stained with AB/PAS of the nasal cavity from various exposure patterns. Nasal transitional epithelium (e) is denoted by blue dash circles, and the mucosubstances are indicated by red arrowheads.

bacteria "curled up" to adhere to the spherical SiO_2 and microplastic particles. Thereafter, the different interactions between the surface of the model FPMs and the membrane of *P. aeruginosa* (i.e., Gram-negative bacteria), namely, the adsorption Coulomb energy and the adsorption van der Waals energy, were calculated through the MD simulations. The adsorption energies between FPMs and bacteria were negative, reflecting the thermodynamic feasibility of bacterial adsorption to FPMs (Figure S2). In addition, the various surfaces showed different adsorption abilities to bacteria. In specific, the adsorption energies of bacteria to Al_2O_3 were much lower than those to SiO_2, indicating that the bacteria stayed more stable on the surface of Al_2O_3 than SiO_2. It should be noted that the different interaction patterns between FPMs

https://doi.org/10.1021/acs.est.2c03856
Environ. Sci. Technol. 2022, 56, 15892−15901

and bacteria largely depended on the surface properties of FPMs and may further affect the viability and invasion of the adherent bacteria.[22,42,43]

Then, the invasive ability of co-exposure (i.e., FPMs and *P. aeruginosa*) was examined. The treatment of FPMs did not induce detectable cytotoxicity to the cell and bacteria using the currently available toxicity assays (Figures S3 and S4). In general, the co-exposure of FPMs and *P. aeruginosa* increased the invasive ability of *P. aeruginosa*, as shown in Figure 1F−J. Moreover, various FPMs exhibited different enhancements in the invasion of *P. aeruginosa*. For instance, the spherical SiO_2 and FPS particles significantly increased the invasive ability of *P. aeruginosa* (Figure 1G,I). Intriguingly, the invasion ability of *P. aeruginosa* loaded on the FPMs was correlated with the combined adsorption energies (namely, the Coulomb energy combined with the van der Waals energy, Figure S5). The lower adsorption energy of bacteria onto the surface pinpointed the stronger interactions between the FPMs and bacterial membranes, which retarded the movement and invasion ability of the adherent bacteria. The adherent bacteria tended to scratch onto the FPMs instead of translocating from the FPMs into cells. In addition, the smooth surface may provide more binding sites for bacteria and then enhance the accessibility of bacteria to the cells. On the contrary, the rough surface of dust and Al_2O_3 particles cannot provide enough binding sites, and the increase in invasion was much less than that of spherical particles (Figure 1F,J). To confirm the accessibility of bacteria to cells, bacterial adhesion to A549 cells after co-exposure was further evaluated (Figure S6). The FPMs significantly increased the adherence of *P. aeruginosa* to A549 cells. In specific, the adherent bacteria on different FPMs exhibited the corresponding invasive ability. Thus, the results supported that the co-exposure of FPMs and bacteria obviously enhanced the accessibility of *P. aeruginosa* to cells and, thereafter, increased the possibility of infection.

Typically, the spread and biological accessibility of bacteria could be enhanced through hitchhiking onto FPMs. For instance, it has been reported that the FPMs could enter the respiratory tract, and the ultrafine particles could even enter deep into the lung and cross the air−blood barrier.[3,4,44] Specifically, the FPMs have been found in the human serum, pleural effusion, heart tissue, vascular inflammation, brain, knee joint, and placenta.[45−51] Thus, the hitchhiking bacteria might translocate to deeper respiratory tract through adhering to the FPMs and then increase the accessibility and infective possibility to the lung and even the extra-pulmonary organs. However, the possibility is largely dependent on the concentration of airborne bacteria, and it seems to usually occur in indoor environments, for example, hospitals.[18] It should also be noted that exposure to FPMs could increase the vulnerability of cells and make cells defenseless to pathogens.[27,28] Therefore, the co-exposure of FPMs and bacteria significantly increased the accessibility of *P. aeruginosa* and inhibited the resistance of epithelial cells, which further led to higher invasion of bacteria.

Laboratory Co-Exposure Model Setup and the Influence on the Nasal Cavity. As previously stated, it has been proposed that FPMs impair the functions of the inhalation system via inducing oxidative stress, which further increase the infection efficiency of pathogens.[28] However, because of the deficiency of the exposure patterns, limited studies have discussed the co-exposure of FPMs and pathogens, as well as the related health effects. Here, to better imitate a real co-exposure scenario, we designed and constructed a chamber for animal experiments, as shown in both the photograph and scheme (Figure 2). The animals could be exposed to variable FPMs under different concentrations and different pathogens (e.g., bacteria, fungi, and viruses), which warrants further investigation in the future studies. It should also be noted that this laboratory model made the interaction between FPMs and pathogens more effective than that in the real atmosphere environment.

To better imitate a real PM exposure, we used SiO_2 particles (a major component in the real dust sample) as a representative of FPMs. The BALB/c mice (male, 6−7 weeks old, 20 g for average weight) were exposed to single FPMs (i.e., SiO_2 particles), single bacteria, or the co-exposure experiment for 30 min. After that, to examine the transmission ability of bacteria loading on the FPMs, the nasal wash of the mice exposed to particles combined with bacteria and bacteria only were collected. The bacterial loads in nasal wash were then evaluated. Intriguingly, co-exposure significantly increased the bacterial loads in the nasal cavity, compared with the bacteria-only exposure (Figure 3A,B). The results indicated the possible "vehicle" properties of FPMs, that is, to carry and facilitate the bacteria to enter the nasal cavity as well as the whole upper respiratory tract. Intriguingly, co-exposure seemed to accelerate the clearance of the nasal tract (namely, the innate protection mechanism of the body), as there was a significant decrease (approximately 50%) in CFU counts in the nasal wash quickly within 3 h after exposure (Figure 3A). However, whether the invaders were cleared or translocated to the trachea could not be defined. In contrast, the exposure of bacteria only induced slower clearance because there was no significant decrease in CFU counts at 3 h (Figure 3B). The results eventually indicated the significant stimuli of inhaled FPMs on the upper respiratory tract, corresponding to previous studies.[26] In addition, most of the bacterial loads in the nasal cavity would be cleared in 24 h after both exposure because of physical and immune clearance by epithelial structures because there was no bacterium detected in nasal wash (Figure 3A,B).[52]

Thereafter, the nasal histopathology was examined after various exposure patterns. As a consequence, there was a significant increase in the thickness of the nasal transitional epithelium (e) (Figure 3C). In specific, co-exposure induced a much higher increase in the thickness of the nasal transitional epithelium, that is, 19.23 μm, compared with the 7.23 μm thickness of the untreated control. Moreover, while the thickness of the nasal transitional epithelium after particle exposure and bacteria exposure also increased, to 9.27 and 12.84 μm, respectively, the thickness of the nasal transitional epithelium upon co-exposure showed the highest increase. The nasal transitional epithelium is the first and an important defense of the upper respiratory tract that protects the body from potentially dangerous inhaled particles and pathogens.[52] The thicker nasal transitional epithelium indicated hyperplasia and hypertrophy of epithelial cells after exposure.[53] Specifically, there was a marked inflammatory cell influx in the lamina propria of the nasal mucosa after co-exposure (yellow arrowheads showed), indicating an inflammatory reaction after co-exposure treatment. In addition, the nasal histopathology was examined after exposure for 3 h. The nasal transitional epithelium was still thicker than that of the untreated control after co-exposure, indicating long-term effects on the nasal cavity (Figure S7).

https://doi.org/10.1021/acs.est.2c03856
Environ. Sci. Technol. 2022, 56, 15892−15901

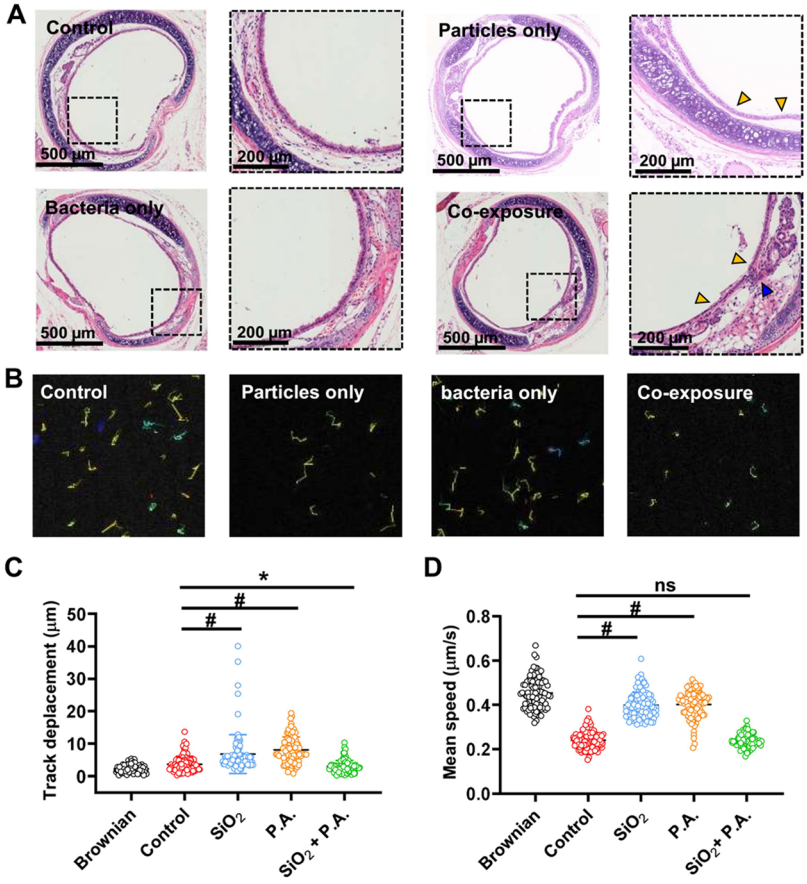

Figure 4. Histology and physiology of the trachea structure after various exposure patterns. (A) Histology stained with H&E of the trachea from mice exposed to clean air, FPMs-only, bacteria-only, and co-exposure for 30 min. The cilia structure is denoted by yellow arrowheads, and the inflammatory cell influx is indicated by blue arrowheads. (B−D) Different exposure patterns affected MCC. (B) Representative projected images of labels diffusion over a span of 0.03 s. (C,D) Distance and speed of cilia-generated flow are measured by multiple particle tracking. Statistical significance between groups: (*) $P < 0.05$ and (#) $P < 0.001$. NS represents no significance between the two groups.

Furthermore, the staining for AB/PAS-positive mucous cells and mucosubstances was examined. The mucosubstances significantly increased after all treatments, indicating the induction of physical defense in the nasal cavity to clear the exotic invaders (Figure 3D).[53] Of note, co-exposure induced the highest increase in mucosubstances compared with other treatments, indicated by the intensity of the darkened blue color. In addition, the thickened nasal epithelium in mice exposed to particle and combined treatment could be notified (blue circles), corresponding to the H&E results. In addition, the density of intraepithelial mucosubstances increased upon particle-only and co-exposure, compared to the untreated control and bacteria-only, as shown by red arrowheads (Figure 3D). These results correlated with the reaction upon particle invasion and clearance. Otherwise, 3 h after exposure, the mucosubstances under co-exposure still exhibited the highest intensity, especially compared with the particle-exposure-only group (Figure S8), in analogy to the higher bacterial loading after 3 h (Figure 3A).

Our results clearly presented the states of bacteria, that is, free bacteria and bacteria loading on the FPMs had effects on the biological availability. Taking advantage of the FPMs, more bacteria could enter the nasal cavity, and then induce more severe reactions. We found a strong reaction of the nasal transitional epithelium and mucosubstances after co-exposure, as more mucosubstances were secreted by mucous cells to clear invaders. However, whether the FPMs and bacteria were cleared by nasal transitional epithelium and mucosubstances, or able to escape from clearance and enter the lower respiratory tract, needs to be further examined.

Co-Exposure of FPMs and Pathogens Impairs the Functionality of the Trachea and MCC. Our data thus far indicated that co-exposure to particles and bacteria could affect the microenvironment of the nasal cavity in specific conditions. Documented by previous studies, FPMs could translocate into the tracheal tissues.[2] Therefore, we examined the histopathology and MCC functionality of the trachea. Compared with the control group, the cilia structures of ciliated cells, which are responsible for clearing exotic pathogens and particles, were damaged after particle-exposure-only and co-exposure (Figure 4A, yellow arrowheads). On the contrary, negligible impairments to ciliated cells were found under the bacteria exposure. In addition, significant inflammatory cell infiltration under the epithelium could also be found after co-exposure (Figure 4A, blue arrowheads). It has been proposed that the impairment of epithelial cells and ciliated cells in the trachea would enhance the invasion of pathogens in the inhalation.[54] Hence, these results suggested that the tissue functions of epithelial cells, especially ciliated cells, were impaired after co-exposure.

Furthermore, the MCC was examined to determine the impact of different exposure patterns. MCC is an important innate defense mechanism that is responsible for removing and

https://doi.org/10.1021/acs.est.2c03856
Environ. Sci. Technol. 2022, 56, 15892−15901

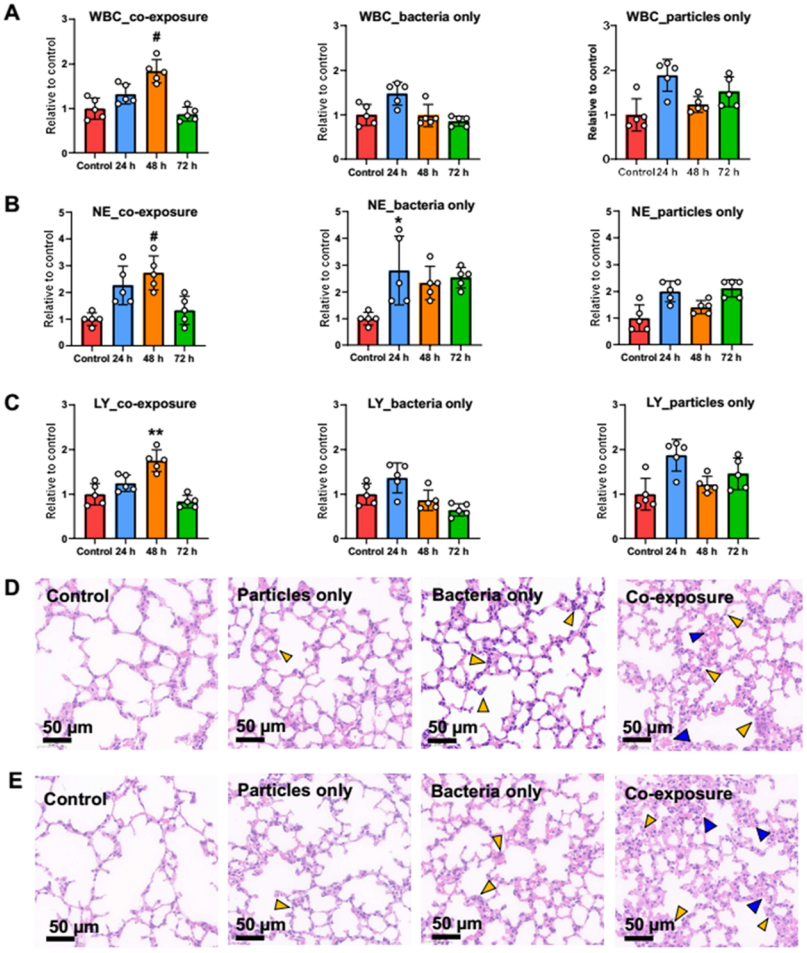

Figure 5. Inflammatory reaction and the histology of the lung after various exposure patterns. Typical inflammatory cells in peripheral blood specimens, that is, WBC (A), NE (B), and LY (C) under different exposure conditions are measured for 72 h after treatment. (D,E) Histology stained with H&E of lungs from mice after exposure to clean air, FPMs-only, bacteria-only, and co-exposure for 0 h (D) and 24 h (E). Infiltration of inflammatory cells is denoted by yellow arrowheads, and the congestion is indicated by blue arrowheads. Statistical significance between groups: (*) $P < 0.05$, (**) $P < 0.05$, and (#) $P < 0.001$.

clearing exotic pathogens, allergens, and particles by ciliary action.[38] Here, we applied a method to determine the impact of different exposure on the function of the MCC.[38,55] It has been proposed that the MCC should increase after exposure to clear inhaled invaders.[55] Hence, tracheal MCC was significantly increased after inhalation exposure in the chamber, indicating that the body innate defense system was stimulated by exotic invaders (Figure 4C,D).[55] Both the track distance and mean speed significantly increased in the trachea of mice after exposure, which reflects the vigorous movement by cilia. In specific, the particle-only exposure increased the moving distance by approximately 45% and the moving speed of cilia by approximately 40% ($P < 0.001$). Exposure to bacteria alone increased the moving distance by approximately 55% and the moving speed of cilia by approximately 40% ($P < 0.001$). The strong movement of cilia after exotic invader exposure pinpointed the fast clearance of the trachea from further damage and infections. Intriguingly, the MCC was severely impaired in the trachea after co-exposure, especially for the moving distance of the cilia. The retarded movements of cilia indicated the functional damage. Therefore, the impaired MCC ability corresponded to the histopathology of the trachea, indicating the damage of the cilia structure, and may cause more serious infections.

The trachea is an important connection between the upper and lower respiratory systems. The impairment of the cilia structures and functions would induce detrimental outcomes, especially pathogen invasions. Previous studies that applied intranasal or intratracheal administration often ignored the influences on the nasal and tracheal parts. Our exposure model demonstrated that the co-exposure of FPMs and loaded bacteria rendered mice more pathological consequences of structural damage and inflammatory activation in the trachea of mice. Moreover, co-exposure impaired the MCC function of the trachea and the tissue repair function of airway epithelial cells.

Co-Exposure of FPMs and Pathogens Predisposes Mice to the Inflammatory Reaction. In addition, we further examined the systematic inflammatory reaction after different exposure patterns. According to the analysis of blood specimens, the co-exposure elicited a more severe inflammatory reaction than the other two single exposures (Figure 5A–C). In specific, the white blood cell (WBC) count of the co-exposure group significantly increased approximately two-fold compared with that of the control group at 48 h and recovered to a normal state at 72 h after exposure, indicating the long inflammatory reaction in mice. Remarkably, the WBC count of the co-exposure group at 48 h was much higher than that of

https://doi.org/10.1021/acs.est.2c03856
Environ. Sci. Technol. 2022, 56, 15892−15901

bacteria-only ($P < 0.001$) and particle-only ($P < 0.01$) groups. Consistently, the neutrophil (NE) and lymphocyte (LY) counts exhibited the same change trends after co-exposure. In addition, the expression of interleukin-6 (IL-6) in sera after exposure also supported the systemic inflammatory reaction in mice (Figure S9). Of note, the inflammatory reaction corresponded to inflammatory cell infiltration in the nasal cavity and trachea after co-exposure. On the contrary, the inflammatory cells in the peripheral blood of the bacteria-only and particle-only groups slightly increased at 24 h after exposure and returned to a normal state at 48 h. The different change trends of the inflammatory cells after exposure pinpointed that the co-exposure would induce a more severe inflammatory reaction in the inhalation system, as well as the immune system of the whole body.

It should be noted that only particles with ultrasmall sizes, namely, the ultrafine particles, could enter deeply in the lungs. Our model FPMs should be cleared by the upper respiratory system. In fact, the lavage fluids from the lung did not contain any bacteria, as confirmed by polymerase chain reaction (PCR) analysis and plate count experiments (data not shown). However, as systematic inflammatory reactions were induced after co-exposure, the indirect influence on the major organ in the respiratory system, that is, the lung, was further examined. The histopathology of the lung was examined right after exposure (i.e., 0 h) and 24 h after exposure (Figure 5D,E). Compared with the untreated control, significant alveolar injury and inflammation coupled with infiltration of inflammatory cells (yellow arrowheads) after various treatments was recognized. In specific, the pronounced congestion was observed after co-exposure (blue arrowheads), revealing the structural damages after co-exposure. Although the FPMs and bacteria did not reach the lower respiratory system, inflammatory injury was induced after exposure. In addition, after 24 h, the inflammation in the lung was still not alleviated and repaired, indicating the long-term injury of the co-exposure (Figure 5E).

The remarkable inflammatory reaction after co-exposure apparently indicated more severe infections of bacterial loading on the FPMs. Moreover, in contrast to previous studies that explicated the damage of FPMs to the respiratory systems, this model revealed the difference in transmission and invasion by bacteria loaded on FPMs, that is to say, the damage and inflammation would be enlarged and prolonged. Of note, although the bacteria loaded on the FPMs may not enter the lung system, the inflammatory reactions induced by the bacteria would evoke the body immune system and then affect the whole respiratory system. In addition, under the same period of exposure, the co-exposure obviously induced more serious reaction in the lung. A heavily inflammatory microenvironment of the lung further induces damage and diseases, such as chronic obstructive pulmonary disease (COPD) and pulmonary fibrosis.[4]

We here reported the health effects of co-exposure of FPM and pathogens, that is, *P. aeruginosa*, on the upper respiratory tract as well as the systematic reaction. Airborne FPMs could load with pathogens, such as bacteria and viruses, while floating and then facilitate pathogen transmission and infection.[3,10] Recent studies have often applied nasal instillation or intratracheal administration to study the health effects of air pollution.[28,30,40,47,56] These exposure methods could simulate inhalation exposure and refer to detrimental outcomes somehow. However, the particles should be suspended in the solution before administration, and this process apparently is not realistic. Therefore, limited by the experimental procedure, previous studies have focused on the impairments to the respiratory systems caused by PM pollution and the defenseless outcomes under pathogen invasion. The separate exposure cannot reflect one process, that is, the FPMs laden with bacteria and then co-exposed to body systems. Hereby, our established model could simulate the exposure of FPMs laden with pathogens simultaneously and reveal a more realistic scenario, which helped us to elicit and explore the related health effects. In specific, the laboratory model made the mixture of pathogens and particles lead to a more effective interaction than that in real-world cases, leading to a better understanding of the co-exposure scenario. It also should be noted that because of the limit data of this study, more efforts could be focus on the differences between various FPMs and even real PM samples, the influences of the particle size and concentration, and the effects after acute and long-term exposure based on experimental periods. Nevertheless, our results uncovered that the pathogens loaded on the FPMs gained more accessibility to the upper respiratory tract and could induce more serious inflammatory and immune reactions. This study thus offers a new point of view to study the health risks of air pollution.

■ ASSOCIATED CONTENT

Supporting Information

The Supporting Information is available free of charge at https://pubs.acs.org/doi/10.1021/acs.est.2c03856.

Additional results of characterization of the bacteria and various FPMs; results of MD simulation; cytotoxicity of FPMs on the A549 cells and bacteria; adherence ability of bacteria to the A549 cells; histology of the nasal cavity after 3 h exposure; and inflammatory reaction after exposure (PDF)

■ AUTHOR INFORMATION

Corresponding Author

Yu Qi − *State Key Laboratory of Environmental Chemistry and Ecotoxicology, Research Center for Eco-Environmental Sciences, Chinese Academy of Sciences, Beijing 100085, China; College of Resources and Environment, University of Chinese Academy of Sciences, Beijing 100049, China;* orcid.org/0000-0002-4862-5347; Email: yuq@rcees.ac.cn

Authors

Yucai Chen − *State Key Laboratory of Environmental Chemistry and Ecotoxicology, Research Center for Eco-Environmental Sciences, Chinese Academy of Sciences, Beijing 100085, China; College of Resources and Environment, University of Chinese Academy of Sciences, Beijing 100049, China*

Xu Yan − *State Key Laboratory of Environmental Chemistry and Ecotoxicology, Research Center for Eco-Environmental Sciences, Chinese Academy of Sciences, Beijing 100085, China; College of Resources and Environment, University of Chinese Academy of Sciences, Beijing 100049, China*

Wei Liu − *State Key Laboratory of Environmental Chemistry and Ecotoxicology, Research Center for Eco-Environmental Sciences, Chinese Academy of Sciences, Beijing 100085,*

https://doi.org/10.1021/acs.est.2c03856
Environ. Sci. Technol. 2022, 56, 15892−15901

China; College of Resources and Environment, University of Chinese Academy of Sciences, Beijing 100049, China

Li Ma − *Aerosol and Haze Laboratory, Advanced Innovation Center for Soft Matter Science and Engineering, Beijing University of Chemical Technology, Beijing 100029, China*

Yongchun Liu − *Aerosol and Haze Laboratory, Advanced Innovation Center for Soft Matter Science and Engineering, Beijing University of Chemical Technology, Beijing 100029, China;* orcid.org/0000-0002-9055-970X

Qingxin Ma − *State Key Laboratory of Environmental Chemistry and Ecotoxicology, Research Center for Eco-Environmental Sciences, Chinese Academy of Sciences, Beijing 100085, China; College of Resources and Environment, University of Chinese Academy of Sciences, Beijing 100049, China*

Sijin Liu − *State Key Laboratory of Environmental Chemistry and Ecotoxicology, Research Center for Eco-Environmental Sciences, Chinese Academy of Sciences, Beijing 100085, China; College of Resources and Environment, University of Chinese Academy of Sciences, Beijing 100049, China;* orcid.org/0000-0002-5643-0734

Complete contact information is available at: https://pubs.acs.org/10.1021/acs.est.2c03856

Notes

The authors declare no competing financial interest.

■ ACKNOWLEDGMENTS

This project was supported by the National Natural Science Foundation of China (Grants 91943301, 21906175, 22150006, 22193051, and 22021003) and the Beijing Natural Science Foundation (Grants 8191002).

■ REFERENCES

(1) The World Health Organization, http://www.euro.who.int/en/home.

(2) Anderson, J. O.; Thundiyil, J. G.; Stolbach, A. Clearing the air: A review of the effects of particulate matter air pollution on human health. *J. Med. Toxicol.* **2012**, *8*, 166−175.

(3) Ma, Q.; Qi, Y.; Shan, Q.; Liu, S.; He, H. Understanding the knowledge gaps between air pollution controls and health impacts including pathogen epidemic. *Environ. Res.* **2020**, *189*, No. 109949.

(4) Xia, T.; Zhu, Y.; Mu, L.; Zhang, Z. F.; Liu, S. Pulmonary diseases induced by ambient ultrafine and engineered nanoparticles in twenty-first century. *Natl. Sci. Rev.* **2016**, *3*, 416−429.

(5) Peixoto, M. S.; de Oliveira Galvão, M. F.; de Medeiros, S. J. R. Cell death pathways of particulate matter toxicity. *Chemosphere* **2017**, *188*, 32−48.

(6) Wang, H.; Yin, P.; Fan, W.; Wang, Y.; Dong, Z.; Deng, Q.; Zhou, M. Mortality risk associated with short-term exposure to particulate matter in China: Estimating error and implication. *Environ. Sci. Technol.* **2021**, *55*, 1110−1121.

(7) Comunian, S.; Dongo, D.; Milani, C.; Palestini, P. Air pollution and Covid-19: The role of particulate matter in the spread and increase of Covid-19's morbidity and mortality. *Int. J. Environ. Res. Public Health* **2020**, *17*, 4487.

(8) Domingo, J. L.; Rovira, J. Effects of air pollutants on the transmission and severity of respiratory viral infections. *Environ. Res.* **2020**, *187*, No. 109650.

(9) Fattorini, D.; Regoli, F. Role of the chronic air pollution levels in the Covid-19 outbreak risk in Italy. *Environ. Pollut.* **2020**, *264*, No. 114732.

(10) Park, E. H.; Heo, J.; Kim, H.; Yi, S. M. The major chemical constituents of $PM_{2.5}$ and airborne bacterial community phyla in Beijing, Seoul, and Nagasaki. *Chemosphere* **2020**, *254*, No. 126870.

(11) Wong, C. M.; Yang, L.; Thach, T. Q.; Chau, P. Y.; Chan, K. P.; Thomas, G. N.; Lam, T. H.; Wong, T. W.; Hedley, A. J.; Peiris, J. S. Modification by influenza on health effects of air pollution in Hong Kong. *Environ. Health Perspect.* **2009**, *117*, 248−253.

(12) Pompilio, A.; Di Bonaventura, G. Ambient air pollution and respiratory bacterial infections, a troubling association: epidemiology, underlying mechanisms, and future challenges. *Crit. Rev. Microbiol.* **2020**, *46*, 600−630.

(13) Belosi, F.; Conte, M.; Gianelle, V.; Santachiara, G.; Contini, D. On the concentration of SARS-CoV-2 in outdoor air and the interaction with pre-existing atmospheric particles. *Environ. Res.* **2021**, *193*, No. 110603.

(14) Lai, T. C.; Chiang, C. Y.; Wu, C. F.; Yang, S. L.; Liu, D. P.; Chan, C. C.; Lin, H. H. Ambient air pollution and risk of tuberculosis: a cohort study. *Occup. Environ. Med.* **2016**, *73*, 56−61.

(15) Liu, Y.; Ning, Z.; Chen, Y.; Guo, M.; Liu, Y.; Gali, N. K.; Sun, L.; Duan, Y.; Cai, J.; Westerdahl, D.; Liu, X.; Xu, K.; Ho, K.-F.; Kan, H.; Fu, Q.; Lan, K. Aerodynamic analysis of SARS-CoV-2 in two Wuhan hospitals. *Nature* **2020**, *582*, 557−560.

(16) Wu, T.; Täubel, M.; Holopainen, R.; Viitanen, A.-K.; Vainiotalo, S.; Tuomi, T.; Keskinen, J.; Hyvärinen, A.; Hämeri, K.; Saari, S. E.; Boor, B. E. Infant and adult inhalation exposure to resuspended biological particulate matter. *Environ. Sci. Technol.* **2018**, *52*, 237−247.

(17) Kvasnicka, J.; Hubal, E. A. C.; Siegel, J. A.; Scott, J. A.; Diamond, M. L. Modeling clothing as a vector for transporting airborne particles and pathogens across indoor microenvironments. *Environ. Sci. Technol.* **2022**, *56*, 5641−5652.

(18) Dinoi, A.; Feltracco, M.; Chirizzi, D.; Trabucco, S.; Conte, M.; Gregoris, E.; Barbaro, E.; La Bella, G.; Ciccarese, G.; Belosi, F.; La Salandra, G.; Gambaro, A.; Contini, D. A review on measurements of SARS-CoV-2 genetic material in air in outdoor and indoor environments: Implication for airborne transmission. *Sci. Total Environ.* **2022**, *809*, No. 151137.

(19) Pivato, A.; Amoruso, I.; Formenton, G.; Di Maria, F.; Bonato, T.; Vanin, S.; Marion, A.; Baldovin, T. Evaluating the presence of SARS-CoV-2 RNA in the particulate matters during the peak of COVID-19 in Padua, northern Italy. *Sci. Total Environ.* **2021**, *784*, No. 147129.

(20) Chirizzi, D.; Conte, M.; Feltracco, M.; Dinoi, A.; Gregoris, E.; Barbaro, E.; La Bella, G.; Ciccarese, G.; La Salandra, G.; Gambaro, A.; Contini, D. SARS-CoV-2 concentrations and virus-laden aerosol size distributions in outdoor air in north and south of Italy. *Environ. Int.* **2021**, *146*, No. 106255.

(21) Conte, M.; Feltracco, M.; Chirizzi, D.; Trabucco, S.; Dinoi, A.; Gregoris, E.; Barbaro, E.; La Bella, G.; Ciccarese, G.; Belosi, F.; La Salandra, G.; Gambaro, A.; Contini, D. Airborne concentrations of SARS-CoV-2 in indoor community environments in Italy. *Environ. Sci. Pollut. Res. Int.* **2022**, *29*, 13905−13916.

(22) Zhang, X.; Li, Z.; Hu, J.; Yan, L.; He, Y.; Li, X.; Wang, M.; Sun, X.; Xu, H. The biological and chemical contents of atmospheric particulate matter and implication of its role in the transmission of bacterial pathogenesis. *Environ. Microbiol.* **2021**, *23*, 5481−5486.

(23) Chen, H.; Du, R.; Zhang, Y.; Du, P.; Zhang, S.; Ren, W.; Yang, M. Evolution of $PM_{2.5}$ bacterial community structure in Beijing's suburban atmosphere. *Sci. Total Environ.* **2021**, *799*, No. 149387.

(24) Fs, A.; Yzb, C.; Mn, A.; Feng, Z. A.; Yan, W. D.; Jw, B.; Tong, Z. B.; Yw, B.; Zw, B.; Min, H. B. J. E. P. Characteristics of biological particulate matters at urban and rural sites in the North China Plain. *Environ. Pollut.* **2019**, *253*, 569−577.

(25) Lu, R.; Li, Y.; Li, W.; Xie, Z.; Fan, C.; Liu, P.; Deng, S. Bacterial community structure in atmospheric particulate matters of different sizes during the haze days in Xi'an, China. *Sci. Total Environ.* **2018**, *637*−*638*, 244−252.

(26) Mushtaq, N.; Ezzati, M.; Hall, L.; Dickson, I.; Kirwan, M.; Png, K. M.; Mudway, I. S.; Grigg, J. Adhesion of Streptococcus pneumoniae to human airway epithelial cells exposed to urban particulate matter. *J. Allergy Clin. Immunol.* **2011**, *127*, 1236−1242.e2.

(27) Chen, X.; Liu, J.; Zhou, J.; Wang, J.; Chen, C.; Song, Y.; Pan, J. Urban particulate matter (PM) suppresses airway antibacterial defence. *Respir. Res.* **2018**, *19*, 5.
(28) Liu, J.; Chen, X.; Dou, M.; He, H.; Ju, M.; Ji, S.; Zhou, J.; Chen, C.; Zhang, D.; Miao, C.; Song, Y. Particulate matter disrupts airway epithelial barrier via oxidative stress to promote Pseudomonas aeruginosa infection. *J. Thorac. Dis.* **2019**, *11*, 2617−2627.
(29) Hoang Bui, V. K.; Moon, J. Y.; Chae, M.; Park, D.; Lee, Y.-C. Prediction of aerosol deposition in the human respiratory tract via computational models: A review with recent updates. *Atmosphere* **2020**, *11*, 137.
(30) Shears, R. K.; Jacques, L. C.; Naylor, G.; Miyashita, L.; Khandaker, S.; Lebre, F.; Lavelle, E. C.; Grigg, J.; French, N.; Neill, D. R.; Kadioglu, A. Exposure to diesel exhaust particles increases susceptibility to invasive pneumococcal disease. *J. Allergy Clin. Immunol.* **2020**, *145*, 1272−1284.e6.
(31) Yadav, M. K.; Go, Y. Y.; Jun, I.; Chae, S. W.; Song, J. J. Urban particles elevated Streptococcus pneumoniae biofilms, colonization of the human middle ear epithelial cells, mouse nasopharynx and transit to the middle ear and lungs. *Sci. Rep.* **2020**, *10*, 5969.
(32) Nivens, D. E.; Ohman, D. E.; Williams, J.; Franklin, M. J. Role of alginate and its O acetylation in formation of Pseudomonas aeruginosa microcolonies and biofilms. *J. Bacteriol.* **2001**, *183*, 1047−1057.
(33) Arizona Test Dust (ATD), https://www.powdertechnologyinc.com/product/iso-12103-1-a1-ultrafine-test-dust/.
(34) Huang, J.; Rauscher, S.; Nawrocki, G.; Ran, T.; Feig, M.; de Groot, B. L.; Grubmüller, H.; MacKerell, A. D., Jr. Charmm36m: An improved force field for folded and intrinsically disordered proteins. *Nat. Methods* **2017**, *14*, 71.
(35) Heinz, H.; Lin, T.-J.; Kishore Mishra, R.; Emami, F. S. Thermodynamically consistent force fields for the assembly of inorganic, organic, and biological nanostructures: The interface force field. *Langmuir* **2013**, *29*, 1754−1765.
(36) Boags, A.; Hsu, P.-C.; Samsudin, F.; Bond, P. J.; Khalid, S. Progress in molecular dynamics simulations of gram-negative bacterial cell envelopes. *J. Phys. Chem. Lett.* **2017**, *8*, 2513−2518.
(37) Jain, A.; Ong, S. P.; Hautier, G.; Chen, W.; Richards, W. D.; Dacek, S.; Cholia, S.; Gunter, D.; Skinner, D.; Ceder, G.; Persson, K. A. Commentary: The Materials Project: A materials genome approach to accelerating materials innovation. *APL Mater.* **2013**, *1*, No. 011002.
(38) Francis, R.; Lo, C. Ex vivo method for high resolution imaging of cilia motility in rodent airway epithelia. *J. Visualized Exp.* **2013**, 78.
(39) Prata, J. C.; da Costa, J. P.; Lopes, I.; Duarte, A. C.; Rocha-Santos, T. Environmental exposure to microplastics: An overview on possible human health effects. *Sci. Total Environ.* **2020**, *702*, No. 134455.
(40) Wei, W.; Yan, Z.; Liu, X.; Qin, Z.; Tao, X.; Zhu, X.; Song, E.; Chen, C.; Ke, P. C.; Leong, D. T.; Song, Y. Brain Accumulation and toxicity profiles of silica nanoparticles: The influence of size and exposure route. *Environ. Sci. Technol.* **2022**, 8319.
(41) Li, D.; Li, Y.; Li, G.; Zhang, Y.; Li, J.; Chen, H. Fluorescent reconstitution on deposition of PM2.5 in lung and extrapulmonary organs. *Proc. Natl. Acad. Sci. U. S. A.* **2019**, *116*, 2488−2493.
(42) Gong, J.; Qi, J.; Beibei, E.; Yin, Y.; Gao, D. Concentration, viability and size distribution of bacteria in atmospheric bioaerosols under different types of pollution. *Environ. Pollut.* **2020**, *257*, No. 113485.
(43) Smets, W.; Moretti, S.; Denys, S.; Lebeer, S. Airborne bacteria in the atmosphere: Presence, purpose, and potential. *Atmos. Environ.* **2016**, *139*, 214−221.
(44) Nemmar, A.; Hoet, P. H. M.; Vanquickenborne, B.; Dinsdale, D.; Thomeer, M.; Hoylaerts, M. F.; Vanbilloen, P. H.; Mortelmans, L.; Nemery, B. Passage of inhaled particles into the blood circulation in humans. *Circulation* **2002**, *105*, 411−414.
(45) Lu, D.; Luo, Q.; Chen, R.; Zhuansun, Y.; Jiang, J.; Wang, W.; Yang, X.; Zhang, L.; Liu, X.; Li, F.; Liu, Q.; Jiang, G. Chemical multi-fingerprinting of exogenous ultrafine particles in human serum and pleural effusion. *Nat. Commun.* **2020**, *11*, 2567.
(46) Calderon-Garciduenas, L.; Gonzalez-Maciel, A.; Reynoso-Robles, R.; Hammond, J.; Kulesza, R.; Lachmann, I.; Torres-Jardon, R.; Mukherjee, P. S.; Maher, B. A. Quadruple abnormal protein aggregates in brainstem pathology and exogenous metal-rich magnetic nanoparticles (and engineered Ti-rich nanorods). The substantia nigrae is a very early target in young urbanites and the gastrointestinal tract a key brainstem portal. *Environ. Res.* **2020**, *191*, No. 110139.
(47) Qi, Y.; Wei, S.; Xin, T.; Huang, C.; Pu, Y.; Ma, J.; Zhang, C.; Liu, Y.; Lynch, I.; Liu, S. Passage of exogeneous fine particles from the lung into the brain in humans and animals. *Proc. Natl. Acad. Sci. U. S. A.* **2022**, *119*, No. e2117083119.
(48) Qi, Y.; Wei, S.; Chen, Y.; Pu, Y.; Liu, S.; Liu, Y. Intrusion of inhaled exotic ultrafine particles into the knee joint in humans and animals: A risk to the joint and surrounding tissues. *Nano Today* **2022**, *43*, No. 101426.
(49) Miller, M. R.; Raftis, J. B.; Langrish, J. P.; McLean, S. G.; Samutrtai, P.; Connell, S. P.; Wilson, S.; Vesey, A. T.; Fokkens, P. H. B.; Boere, A. J. F.; Krystek, P.; Campbell, C. J.; Hadoke, P. W. F.; Donaldson, K.; Cassee, F. R.; Newby, D. E.; Duffin, R.; Mills, N. L. Inhaled nanoparticles accumulate at sites of vascular disease. *ACS Nano* **2017**, *11*, 4542−4552.
(50) Bove, H.; Bongaerts, E.; Slenders, E.; Bijnens, E. M.; Saenen, N. D.; Gyselaers, W.; Van Eyken, P.; Plusquin, M.; Roeffaers, M. B. J.; Ameloot, M.; Nawrot, T. S. Ambient black carbon particles reach the fetal side of human placenta. *Nat. Commun.* **2019**, *10*, 3866.
(51) Calderon-Garciduenas, L.; Gonzalez-Maciel, A.; Mukherjee, P. S.; Reynoso-Robles, R.; Perez-Guille, B.; Gayosso-Chavez, C.; Torres-Jardon, R.; Cross, J. V.; Ahmed, I. A. M.; Karloukovski, V. V.; Maher, B. A. Combustion- and friction-derived magnetic air pollution nanoparticles in human hearts. *Environ. Res.* **2019**, *176*, No. 108567.
(52) Chamanza, R.; Wright, J. A. A review of the comparative anatomy, histology, physiology and pathology of the nasal cavity of rats, mice, dogs and non-human primates. Relevance to inhalation toxicology and human health risk assessment. *J. Comp. Pathol.* **2015**, *153*, 287−314.
(53) Ong, C. B.; Kumagai, K.; Brooks, P. T.; Brandenberger, C.; Lewandowski, R. P.; Jackson-Humbles, D. N.; Nault, R.; Zacharewski, T. R.; Wagner, J. G.; Harkema, J. R. Ozone-induced type 2 immunity in nasal airways. Development and lymphoid cell dependence in mice. *Am. J. Respir. Cell Mol. Biol.* **2016**, *54*, 331−340.
(54) Shahbaz, M. A.; Martikainen, M. V.; Ronkko, T. J.; Komppula, M.; Jalava, P. I.; Roponen, M. Urban air PM modifies differently immune defense responses against bacterial and viral infections in vitro. *Environ. Res.* **2021**, *192*, No. 110244.
(55) Kudo, E.; Song, E.; Yockey, L. J.; Rakib, T.; Wong, P. W.; Homer, R. J.; Iwasaki, A. Low ambient humidity impairs barrier function and innate resistance against influenza infection. *Proc. Natl. Acad. Sci. U. S. A.* **2019**, *116*, 10905−10910.
(56) Wu, B.; Dong, Y.; Wang, M.; Yang, W.; Hu, L.; Zhou, D.; Lv, J.; Chai, T. Pathological damage, immune-related protein expression, and oxidative stress in lungs of BALB/c mice induced by haze $PM_{2.5}$ biological components exposure. *Atmos. Environ.* **2020**, *223*, No. 117230.

https://doi.org/10.1021/acs.est.2c03856
Environ. Sci. Technol. 2022, 56, 15892−15901